increase in propane selectivity was observed as a result of the high amount of propanol added. Propene forms by dehydration of propanol.

The selectivity to 2-methyl-1-alcohols also increased with propanol addition. 2-methyl-1-butanol forms by the condensation of C_1 with 1-butanol and 2-methyl-1-pentanol forms by the self-condensation of 1-propanol. The experiment has to be repeated with the addition of smaller amounts of 1-propanol.

Table 8. Product selectivities and productivities on MG3-13 O/K (1 wt % K-$Cu_{0.5}Mg_5CeO_x$) with and without 1-propanol addition (593 K, 4.5MPa, H_2/CO=1, 3000 cm^3/g-cat·h).

	Without PrOH	with PrOH	Without PrOH
CO Conversion (%)	6.75	5.26	6.30
Rate of Reaction (mmol CO converted/g. cat.*hr.)	3.73	2.90	3.48
Methanol Productivity (g/kg*hr)	70.8	57.3	63.2
Isobutanol Productivity (g/kg*hr)	0.65	7.6	0.98
Selectivities (C%)			
CO_2	21.5	32.7	24.9
Propane(+propene)	4.9	24.4	5.7
methanol	59.3	61.7	56.1
ethanol	2.1	2.4	2.2
isopropanol	4.6	9.3	2.3
unknown	1.8	16.1	1.0
propanol	1.4	-	1.5
2-butanol	0.15	0.85	0.29
isobutanol	0.95	14.0	1.5
1-butanol	0.05	1.24	0.03
2-methyl-1-butanol	0.00	0.77	0.23
1-pentanol	0.08	0.86	0.23
2-methyl-1-pentanol	0.00	4.4	0.00
DME	7.2	2.5	6.8

In the next run Cs-CuZnAl (MG4-2O/Cs) will be tested. This type of catalyst has not been tested at the same conditions as most of K-CuMgCeO catalysts and an "in-house" prepared catalyst of this type has not been tested at all in the CMRU. After this, K-CuMgAl (Mg3-15O/K) and Cs-CuMgAl (Mg3-15O/Cs) will be tested followed by Co- and Pd-promoted modified MgO.

Task 4: Identification of Reaction Intermediates

During this reporting period, a high-pressure catalytic microreactor has been built and attached to the temperature-programmed surface reaction unit for the study of higher alcohol synthesis from CO/H_2. This experiment will focus on the reaction mechanisms for higher alcohol formation especially the chain-growth pathways from C_1 to C_2 alcohols. To fulfill this objective, a mixture of $^{13}CO/H_2$ and CH_3OH will be used as reactants. ^{13}CO contained in a lecture bottle (2.0 MPa) was pressurized using H_2 to make a 1/1 $^{13}CO/H_2$ mixture. This mixture

with a total pressure of 4.0 MPa enables us to run the experiment with a catalyst charge of 1.5 g at 2.0 MPa and a GHSV of 750 cm^3/g-cat-h for 15 h. CH_3OH will be introduced by passing $^{13}CO/H_2$ mixtures through a saturator containing CH_3OH at a desired temperature. All the gas feeding lines after the saturator will be wrapped up with heating tapes to ensure no readsorption and condensation of reactants and products. A part of effluent will be analyzed in-situ by mass spectrometry and the remainder will be trapped and analyzed using GC-MS and liquid-phase NMR.

4.1. Temperature-Program Reduction of MgO-based Cu Catalysts

Temperature-programmed reduction (TPR) was carried out on MgO-based Cu catalysts in order to address the effects of K and CeO_x on the reducibility of CuO. The experiment was carried out by first pretreating the samples at 723 K in flowing He (100 cm^3/min) for 0.5 h to remove carbonates, water, and weakly bonded hydroxyl species. Reactor temperature was then lowered to below 313 K and 5 % H_2/He was introduced at a total flow rate of 100 cm^3/min (STP). The temperature was then increased linearly at a rate of 0.17 K/s and the formation of H_2O and the consumption of H_2 were monitored continuously by mass spectroscopy.

The reduction profiles of MgO-based Cu samples are shown in Figure 14. The onset and peak maximum temperatures for H_2 consumption and H_2O formation obtained on each sample appeared at the same temperature. The high-temperature tail of the H_2O peak is caused by a strong interaction between H_2O and MgO. This tail was not observed for the H_2 peak, but the signal-to-noise ratio of H_2 peak was lower than that of H_2O because of the high H_2 background pressure in the mass spectrometer.

The presence of CeO_x in $Cu_{0.5}Mg_5CeO_x$ decreases the reduction temperature of CuO (508 K to 436 K). CeO_x addition also increases Cu dispersion and decreases Cu particle size, apparently because of the strong interaction between Cu and CeO_x. The large Cu particles in $Cu_{7.5}Mg_5CeO_x$, however, can also be reduced at temperatures lower than on $Cu_{0.1}MgO_x$. The reduction profiles (Figure 14) suggest that the promoting effect of CeO_x on copper oxide reduction is stronger at higher Ce/Mg ratios. CeO_x as a promoter for metal oxide reduction has been reported previously for $Pd/CeO_2/Al_2O_3$ catalysts (13). The presence of CeO_x shifts the reduction temperature of PdO from 437 K to 376 K. Moreover, the reduction behavior of a $Pd/CeO_2/Al_2O_3$ sample prepared by the coprecipitation of Pd and cerium nitrates differs from that of a $Pd/CeO_2/Al_2O_3$ prepared by conventional successive impregnation of CeO_2 and Pd. Some reduction occurs at room temperature on the sample prepared by the coprecipitation methods as a consequence of a higher degree of PdO-CeO_x contact area (14). Lamonier *et al.* (15) have found that Cu^{2+} insertion into CeO_x occurs during the synthesis of $CuCeO_x$ samples by coprecipitation methods. Four different species, present as CuO monomers, dimers, clusters, and small particles have been detected in CuO/CeO_2 mixtures (15).

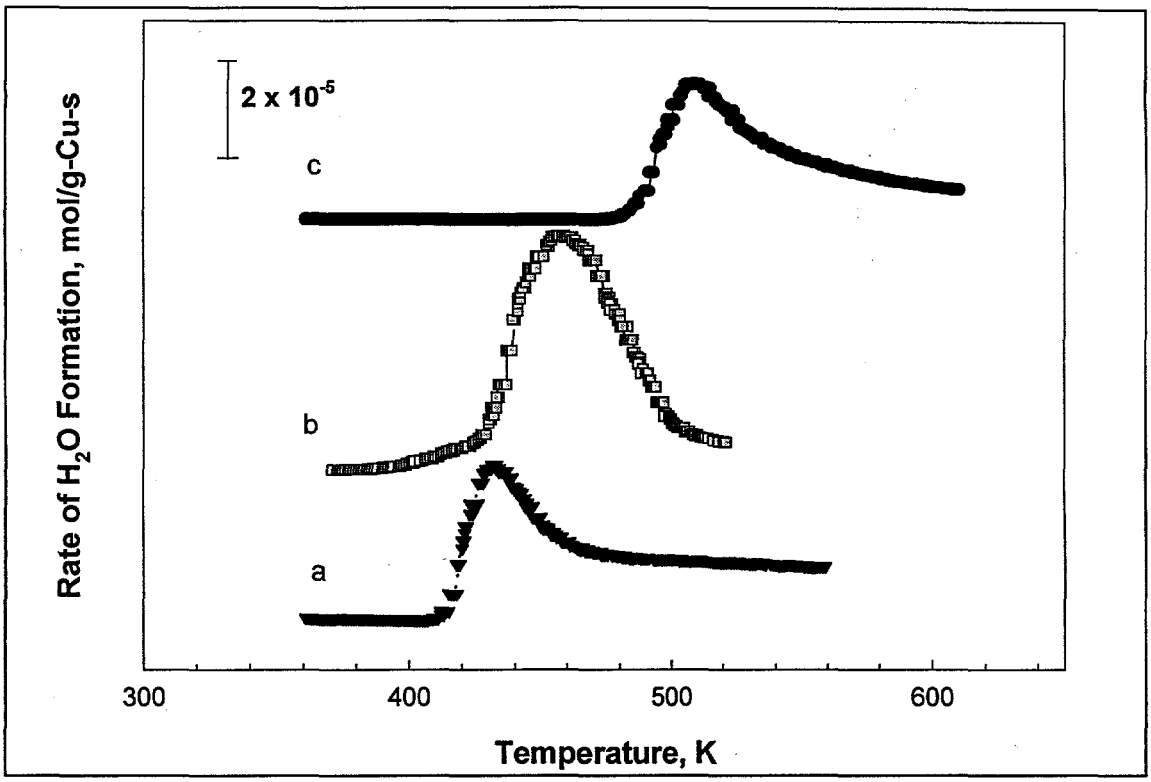

Figure 14. Temperature-programmed reduction profiles obtained in 5 % H_2/He of MgO-based Cu catalysts: (a) $Cu_{0.5}Mg_5CeO_x$; (b) $Cu_{7.5}Mg_5CeO_x$; (c) $Cu_{0.1}Mg_5O_x$. [Heating rate: 0.17 K/s; 15-100 mg of sample, 100 cm^3/min 5% H_2/He mixture; pretreatment temperature: 723 K]

ZnO has an effect similar to that of CeO_x on copper reduction. Garcia-Fierro *et al.* (14, 16) reported that the fraction of copper oxide strongly interacting with ZnO increases with increasing Zn/Cu ratio and that such copper oxide species showed the highest reducibility. A kinetic model of reduction kinetics of CuO/ZnO suggests that the promoting effect of ZnO on copper reduction is caused by the dissociative adsorption of H_2 on ZnO surfaces or on Cu metal clusters closely associated with ZnO (17). The spillover of the hydrogen atoms formed increases the rate of Cu^{2+} reduction. In fact, kinetic analysis showed that the apparent activation energy, E_a, was 84 kJ/mol for the reduction of pure CuO whereas E_a decreased to 77 kJ/mol for the reduction of the CuO-ZnO catalysts (14), in agreement with the promoting effect of ZnO on the reducibility of CuO. Similar processes are likely to occur during CuO reduction on $CuMgCeO_x$ samples. A better contact between CeO_x and Cu is expected with increasing CeO_x/Cu ratio, leading to CuO reduction at lower temperatures.

In contrast to CeO_x, K addition to Cu-containing samples inhibits CuO reduction, as shown by the shift of the reduction peak to higher temperatures (Figure 15). The effect of K is more pronounced on low-Cu ($Cu_{0.5}Mg_5CeO_x$) than on high-Cu ($Cu_{7.5}Mg_5CeO_x$) catalysts (ΔT = 79 K on the former compared to 57 K on the latter). Also, the effect of K was not influenced by the presence of CeO_x; the reduction temperatures increased by approximately the same amount (ΔT = 70 K) on K-$Cu_{0.5}Mg_5O_x$ and K-$Cu_{0.5}Mg_5CeO_x$. K appears to increase the stability of Cu^{2+} ions and make them more difficult to reduce by H_2. A similar effect has been reported on Cs-promoted $Cu/ZnO/Cr_2O_3$ (12). In this study, the presence of Cs retards CuO reduction by about

50 K. Klier and co-workers [12] suggest that the inhibited reduction of CuO is associated to closer interaction between the CuO and promoter phases which inhibited to some extent H_2 activation.

The inhibition effect of K on copper reduction observed in this study can be explained by the inhibited activation of H_2 proposed by Klier and co-workers (12) or by the strengthening of Cu-O bonds upon K addition. As reported in the literature (18, 19), the bond energy of surface oxygen for CuO is about 42 kJ/mol and it increases to 63 kJ/mol upon the addition of 10-25 at. % MgO. Addition of MgO weakens the Cu-Cu bonds and strengthens Cu-O bonds. In a similar way, the incorporation of K_2O into CuO during catalyst synthesis may increase the bond strength of Cu-O and therefore retard CuO reduction.

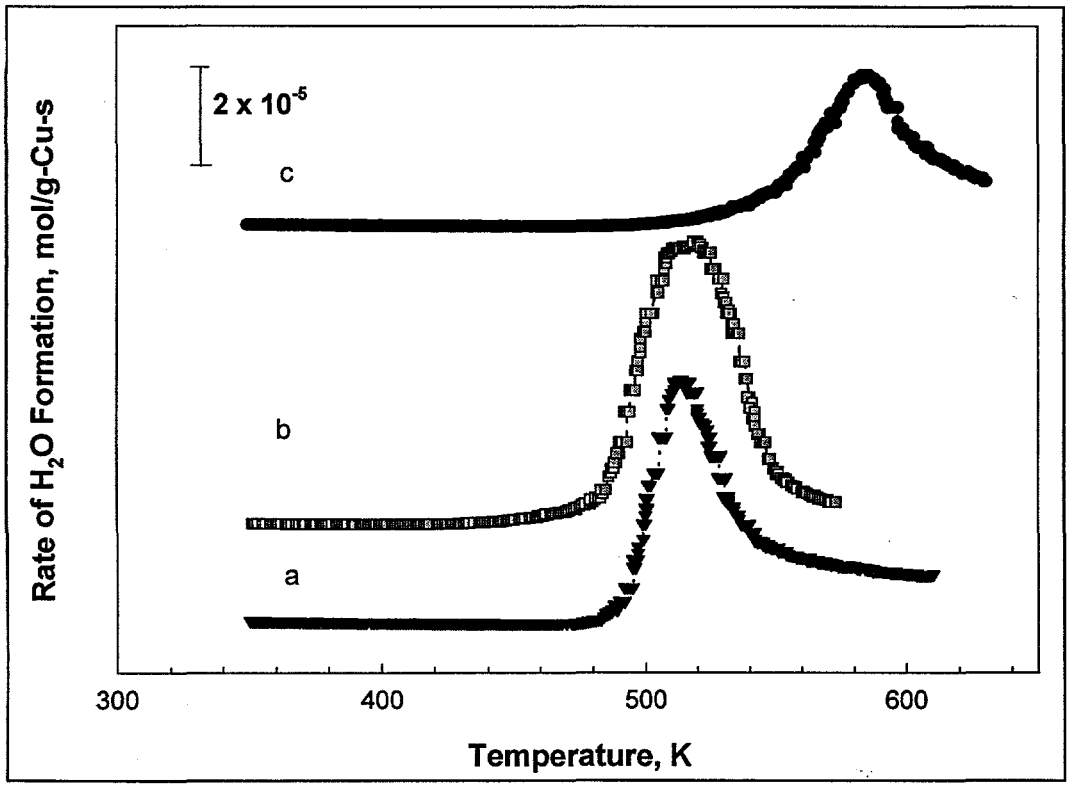

Figure 15. Temperature-programmed reduction profiles obtained in 5 % H_2/He of MgO-based Cu catalysts: (a) 1.0 wt % K-$Cu_{0.5}Mg_5CeO_x$; (b) 1.2 wt % K-$Cu_{7.5}Mg_5CeO_x$; (c) 1.1 wt % K-$Cu_{0.1}Mg_5O_x$. [Heating rate: 0.17 K/s; 15-100 mg of sample, 100 cm^3/min 5% H_2/He mixture; pretreatment temperature: 723 K]

4.2. Determination of Copper Surface Area

The decomposition of N_2O was used to measure Cu surface area of MgO-based Cu Catalysts. In a typical experiment, the catalyst was first reduced at 623 K in flowing H_2 (5 % H_2/He). After reduction, the reactor temperature was lowered to 363 K in flowing He and N_2O decomposition was then conducted via N_2O pulse injections. The Cu surface area was 28.5 m^2/g-cat (Cu dispersion: 6.8 %) for $CuZnAlO_x$ and 23.5 m^2/g (Cu dispersion: 5.2 %) for Cs-

$CuZnAlO_x$, suggesting the addition of Cs to $CuZnAlO_x$ decreases the number of surface exposed Cu atoms. The decrease in Cu surface area upon Cs addition could be due to a decrease in total surface area (from 74 to 62 m^2/g) and blocking of surface Cu by Cs_2CO_3.

The Cu surface area was found to be 13.1 m^2/g-cat (Cu dispersion: 15.8 %) on 1.0 wt % K-$Cu_{0.5}Mg_5CeO_x$ (MG3-13 o/K). The 15.8 % of Cu dispersion on MG3-13 o/K is comparable with the value of 14.1 % obtained on MG-11 ow/K (1.0 wt % K-$Cu_{0.5}Mg_5CeO_x$), suggesting the reproducibility in catalyst preparation. MG3-13 o/K and MG3-11 o/K have the same catalytic compositions but are prepared at different time.

In a typical CMRU experiment, the catalyst deactivates with time on stream. Cu surface area of the used sample (1.0 wt % K-$Cu_{0.5}Mg_5CeO_x$) was determined in order to address the effect of high-pressure catalytic reactions on Cu surface area. The used sample was first treated in flowing He at 723 K for 20 min followed by H_2 reduction at 623 K for 30 min before N_2O titration commenced at 363 K. The copper dispersions on the used 1.1 wt % K-$Cu_{0.5}Mg_5CeO_x$ taken from the top and middle-bottom of the CMRU catalyst bed were 3.6 % and 1.2 %, respectively. The smaller value in the latter suggests that the front part of the catalyst bed in the CMRU reactor is less severely deactivated. It should be pointed out that the total surface areas of these two used samples are comparable. The Cu dispersion of the used sample, however, was much less than that of the fresh sample (15.8 %). The decrease in Cu during reaction is due to 1) a decrease in the total surface area (150 m^2/g to 80 m^2/g) 2) deposition of hydrogen deficient hydrocarbon species on the catalyst surface, and 3) Cu metal sintering during the reaction.

In another experiment, the used 1.0 wt % K-$Cu_{0.5}Mg_5CeO_x$ removed from the top of CMRU reactor was treated in flowing O_2 (5 % O_2/He) instead of He at 723 K. This treatment leads to a Cu dispersion of 20.6 % that is even greater than the fresh sample even though the total surface area of the used sample is still approximately one-half of the fresh sample, suggesting that oxygen treatment at 723 K is able to remove all the species covering on Cu metal atoms. Moreover, alcohol (ROH) and water formed during the reaction could react with surface K^+ ions to form RO^-K^+ and KOH. The loss of RO^-K^+ and water from surface to gas phase results in a loss of surface K^+ ions and an increase in the exposed surface Cu atoms.

4.3 *Determination of Basic Site Density and Strength*

The density of basic sites was determined using a $^{13}CO_2/^{12}CO_2$ exchange method developed as part of this project; this method provides a direct measure of the number of basic sites *"kinetically available" at reaction conditions*. In addition, this technique provides a measure of the distribution of reactivity for such basic sites. In this method, a pre-reducecd catalyst is exposed to a 0.1 % $^{13}CO_2$/0.1 % Ar/He stream and after $^{13}CO_2$ reached a constant level in the effluent, the flow is switched to 0.1 % $^{12}CO_2$/He 573 K. The relaxation of the $^{13}CO_2$ removed from the surface is followed by mass spectrometry and the result obtained on 1.0 wt % K-$Cu_{0.6}Mg_5Ce_{1.2}O_x$ catalyst (MG3-13 o/K) is shown in Figure 16. The presence of Ar permitted the correction for gas-phase holdup and hydrodynamic delays. The exchange capacity at 573 K is calculated from the areas of the $^{13}CO_2$ and Ar peaks. The number of available basic sites in MG3-13 o/K (1.0 wt % K-$Cu_{0.5}Mg_5CeO_x$) is 1.85 x 10^{-6} mol/m^2, which is comparable to the amount (2.33 x 10^{-6} mol/m^2) obtained on MG3-11 ow/K (1.0 wt % K-$Cu_{0.5}Mg_5CeO_x$). This

suggests the reproducibility in catalyst preparation. Weakly interacting sites are mostly unoccupied by CO_2 and strongly interacting sites do not exchange in the time scale of the isotopic relaxation experiment. Neither strongly interacting nor weakly interacting sites are likely to contribute to catalytic reactions at similar temperatures.

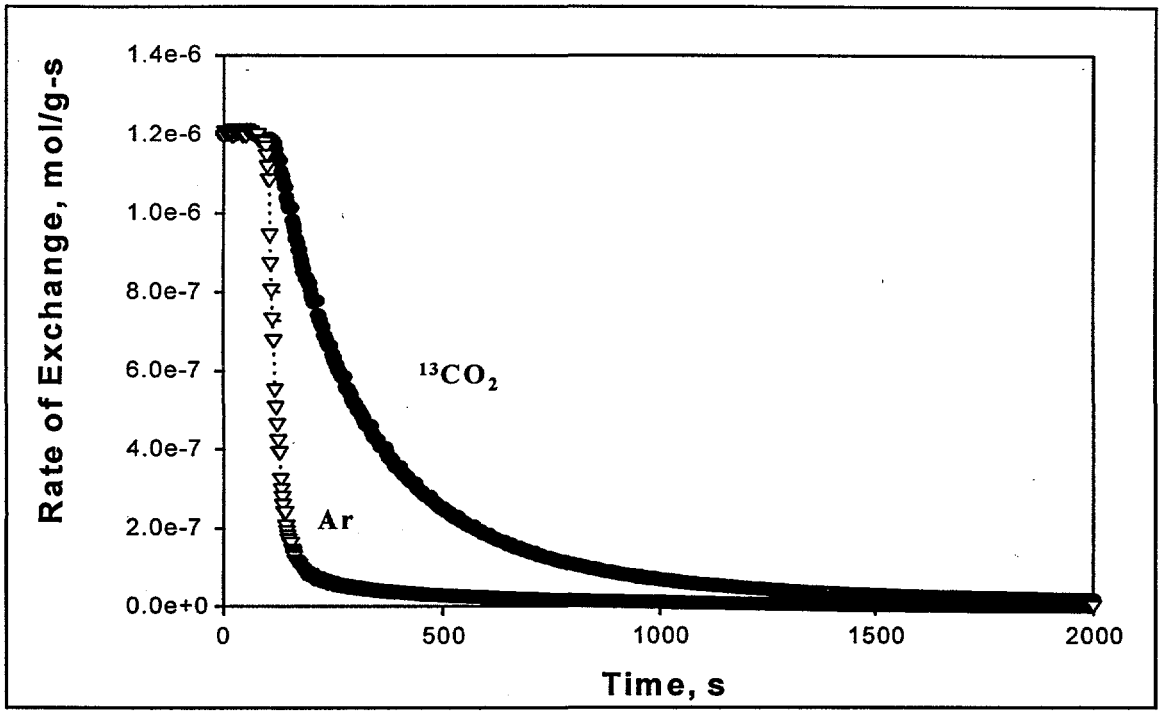

Figure 16. The transient response observed for 1.0 wt % K-$Cu_{0.6}Mg_5Ce_{1.2}O_x$ (MG3-13 o/K) upon switching from $^{13}CO_2$ to $^{12}CO_2$: T = 573 K.

In the experiment mentioned above, the number of available basic sites at 573 K was determined at a total gas flow rate of 100 cm^3/min with 50 mg catalyst charge. We explored the effect of carrier gas flow rate on shapes of the $^{13}CO_2$ transient curves in order to determine the significance of readsorption. In this experiment, three different flow rates (50, 100, and 200 cm^3/min) were used with the amount of catalyst (MG3-11 oW/K, 50 mg) remained unchanged. The number of available basic sites on 1.1 wt % K-$Cu_{0.5}Mg_5CeO_x$ (MG3-11 oW/K) at 573 K determined at these flow rates are comparable (1.8 ± 0.1 mol/m^2). The slopes of these curves, however, increases with increasing flow rates (Figure 7). As one can tell from the mathematical treatment (see Appendix), the gas phase concentrations of desorption products appear to depend on the rates of both desorption and carrier gas flow. The curve slope is a function of desorption rate constant (k_a), adsorption rate constants (k_d), and gas residence time (tr).

$$C_A(t)=C_{Ao}\cdot\frac{\frac{1}{\tau}-k_a}{\frac{1}{\tau}+k_a}-\frac{\theta_o}{\xi}\cdot\exp\left[\left(k_a-k_d+\frac{1}{\tau}\right)\cdot t\right]+\left[C_o-C_{Ao}\cdot\frac{\frac{1}{\tau}-k_a}{\frac{1}{\tau}+k_a}+\frac{\theta_o}{\xi}\right]\cdot\exp\left[-\left(\frac{1}{\tau}+k_a\right)\cdot t\right]$$

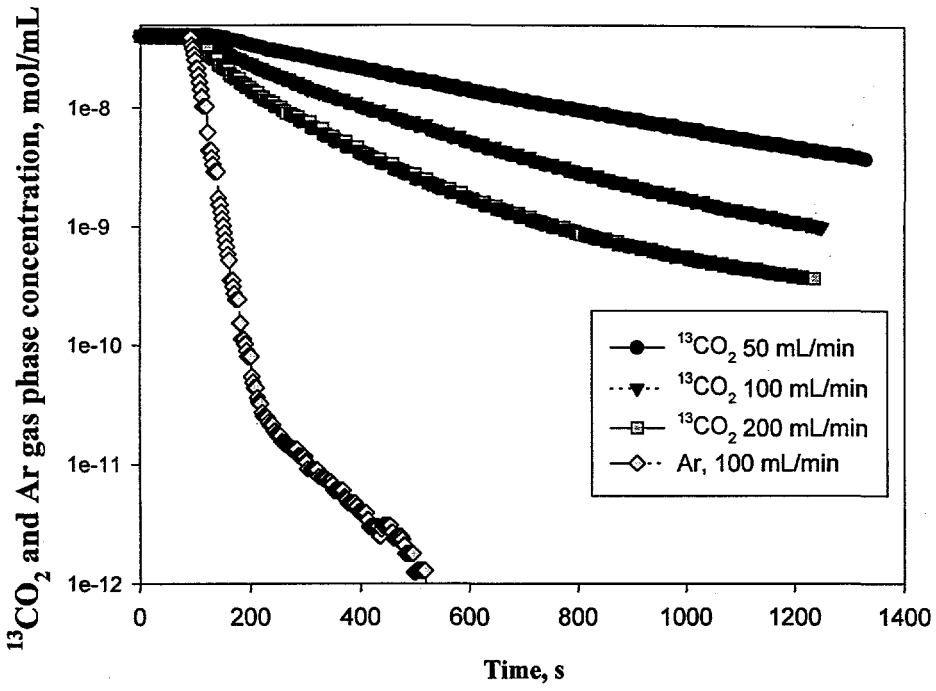

Figure 17. Effect of carrier gas flow rate on the shape of $^{13}CO_2$ transient curve on 1.1 wt% K-$Cu_{0.5}Mg_5CeO_x$ catalysts at 573 K.

Task 5: Bench Scale Testing at Air Products and Chemicals

Activities during this reporting period include meeting with Dr. Bernard A. Toseland from Air Products and Chemicals at Berkeley.

Staffing Plans

No changes.

Other activities

The manuscript *"Isobutanol and Methanol Synthesis on Copper Catalysts Supported on Modified Magnesium Oxide"* has been submitted to Journal of Catalysis for publication. A manuscript entitled *"Isotopic Switch Methods for the Characterization of Basic Sites in Modified MgO Catalysts"* is in the final draft and will be submitted for publication during the next reporting period.

Two abstracts *"Synthesis of Branched Alcohols on Bifunctional (Metal-Base) Catalysts Based on MgO Modified by CeO_x and Copper"* (M.J. Gines, M. Xu, A.M. Hilmen, B. Stephens, and E. Iglesia) and *"An Isotopic Swich Method for the Characterization of Basic Sites in Solids"* (M. Xu, Z. Hu, and E. Iglesia) were submitted to the 15th North American Meeting of the Catalysis Society.

A seminar (*"Reaction Pathways and Catalyst Requirements in the Synthesis of Isobutanol from CO and H_2 on K-CuMgCeO$_s$"*) was presented by Dr. M. Xu at the UOP Research Center.

References

1. Keim, W. and Falter, W., *Catal. Lett.* **3,** 59 (1989).
2. Dombeck, B.D., Heterogeneous Catalytic Process for Alcohol Fuels from Syngas, DOE Contract N° DE-AC 22-91PC90046, Final Technical Report, March 1996.
3. Elliot, D.J. and F. Penella, *J. Catal.* **119** (1989) 359.
4. Nunan, J.G., Bogdan, C.E., Klier, K., Smith, K., Young, C., and Herman, R., *J. Catal.* **116,** 195 (1989).
5. Klier, K., Chatikavanij, V., Herman, R.G., and Simmons, G.W., *J. Catal.,* **74,** 343 (1982).
6. Owen, G., Hawkes, C.R., Lloyd, D., Jennings, J.R., and Lambert, R.M., and Nix, R.M., *Appl. Catal.* **53,** 405 (1987).
7. Pan, W.X., Cao, R., Roberts, D.L., Griffin, G.L., J. Catal. 114 (1988) 440-446.
8. Hoppener, R.H., Doesburg, E.B.M., Scholten, J.J.F., App.Catal. (1986)109-119.
9. Chinchen,, G.C., Waugh, K.C., Whan, D.A., App. Catal. 25 (1986) 101-107.
10. Robbins, J.L., Iglesia, E., Kelkar, C.P., DeRites, B., Catal. Lett. 10 (1991) 1-10.
11. US patent 5,387,570.
12. Campos-Martin, J.M., Fierro, J.L.G., Guerrero-Ruiz, A., Herman, R.G., Klier, K., J. Catal. 163 (1996) 418-428.
13. Souza-Monteiro, R., Noronha, F.B., Dieguez, L.C., and Schmal, M., *Appl. Catal.* **131,** 89 (1995).
14. Garcia-Fierro, J.L., Lo Jacono, M., Inversi, M., Porta, P., Cioci, F., and Lavecchia, R., *Appl. Catal.* **137,** 327 (1996).
15. Lamonier, C., Bennani, A., Duysser, A., and Wrobel, G., *J. Chem. Soc., Faraday Trans.,* **92(1),** 131 (1996).
16. Garcia-Fierro, J.L., Lo Jacono, M., Inversi, M., Porta, P., Lavecchia, R., and Cioci, F., *J. Catal.* **148,** 709 (1994).
17. Annesini, M.C., Lavecchia, R., Marrelli, L., Lo Jacono, M., Campa, M.C., Garcia-Fierro, J.L., Moretti, G., and Porta, P., *Solid State Ionics.* **63-65,** 281 (1993).
18. Davydova, L.P., Boreskov, G.K., Popovskii, V.V., Yurieva, T.M., and Anufrienko, V.F., *React. Kinet. Catal. Lett.* **18,** 203 (1981).
19. Aleksandrov, V.Yu., Popovskii, V.V., and Bulgakov, N.N., *React. Kinet. Catal. Lett.* **8,** 65 (1978).

4. PARTICIPATING PROJECT PERSONNEL

Mingting Xu
Postdoctoral Fellow

Marcelo J. L. Gines
Postdoctoral Fellow

Anne-Mette Hilmen
Postdoctoral Fellow

Zhengjie Hu
Undergraduate Researcher

Bernard A. Toseland
Sub-Contractor
Air Products and Chemicals

Enrique Iglesia
Principal Investigator

Appendix

Mathematical treatment of relaxation profile of $^{13}CO_2$ from catalyst surface

Nomenclature:

N_A	Moles of $^{13}CO_2$	Wg	Weight of catalysts (g)
F_{Ao}	Inlet $^{13}CO_2$ molar flow rate (mol/s)	V	Reactor volume (cm^3)
F_A	Outlet $^{13}CO_2$ molar flow rate (mol/s)	S_A	Catalyst surface area (m^2/g)
C_A	Outlet $^{13}CO_2$ concentration (mol/cm^3)	rt	Residence time (s)
C_{Ao}	Inlet $^{13}CO_2$ concentration (mol/cm^3)	v	Volumetric flow rate (cm^3/s)
θ	$^{13}CO_2$ surface concentration (mol/m^2)	k_d	Desorption rate constant (s^{-1})
θ_0	$^{13}CO_2$ initial surface concentration (mol/m^2)	k_a	Readsorption rate constant (s^{-1})
C_0	Total gas phase concentration (mol/cm^3)		

From mass balance, we get:

$$\frac{dN_A}{dt} = \left(F_{Ao} - F_A\right) + k_d \cdot \theta \cdot S_A \cdot W_g - k_a \cdot C_A \cdot V$$

$$V \cdot \frac{dC_A}{dt} = \left(C_{Ao} \cdot v - C_A \cdot v\right) + k_d \cdot \theta \cdot S_A \cdot W_g - k_a \cdot C_A \cdot V$$

$$\frac{dC_A}{dt} = \frac{C_{Ao} - C_A}{\tau} + \frac{k_d \cdot \theta \cdot S_A \cdot W_g}{V} - k_a \cdot C_A$$

Two coupled differential equations to be solved are as follows:

$$\frac{dC_A}{dt} = \frac{C_{Ao} - C_A}{\tau} + k_d \cdot \theta \cdot S_A \cdot \frac{W_g}{V} - k_a \cdot C_A$$

$$\frac{d\theta}{dt} = \frac{k_a \cdot C_A \cdot V}{S_A \cdot W_g} - k_d \cdot \theta$$

Simplify the above equations:

$$\frac{dC_A}{dt} + \left(\frac{1}{\tau} + k_a\right) \cdot C_A - \frac{S_A \cdot W_g}{V} \cdot k_d \cdot \theta = \frac{C_{Ao}}{\tau}$$

$$\frac{d\theta}{dt} - \frac{V}{S_A \cdot W_g} \cdot k_a \cdot C_A + k_d \cdot \theta = 0$$

let $$\xi = \frac{V}{S_A \cdot W_g}$$

Plugging in:

$$\frac{dC_A}{dt} + \left(\frac{1}{\tau} + k_a\right)\cdot C_A - \frac{k_d}{\xi}\cdot\theta = \frac{C_{Ao}}{\tau}$$

$$\frac{d\theta}{dt} - \xi\cdot k_a \cdot C_A + k_d\cdot\theta = 0$$

Divide the second equation by εk_a

$$\left[D + \left(\frac{1}{\tau} + k_a\right)\right]\cdot C_A - \frac{k_d}{\xi}\cdot\theta = \frac{C_{Ao}}{\tau}$$

$$-C_A + \left(\frac{k_d + D}{\xi\cdot k_a}\right)\cdot\theta = 0$$

Do operation , $(D+1/\tau+k_d)$, on the 2nd equation and add it to the first equation to get a new 2nd equation:

$$\left[D + \left(\frac{1}{\tau} + k_a\right)\right]\cdot C_A - \frac{k_d}{\xi}\cdot\theta = \frac{C_{Ao}}{\tau} \qquad (1)$$

$$\left[\frac{-k_d}{\xi} + \left(\frac{k_d}{\xi\cdot k_a} + \frac{D}{\xi\cdot k_a}\right)\cdot\left[D + \left(\frac{1}{\tau} + k_a\right)\right]\right]\cdot\theta = \frac{C_{Ao}}{\tau} \qquad (2)$$

Now the 2nd equation is only in terms of θ only. It is just a second order nonhomogenuous differential equation. Simplifying (2) we get:

$$\left[D^2 + \left(k_d + k_a + \frac{1}{\tau}\right)\cdot D + \frac{k_d}{\tau}\right]\cdot\theta = \frac{C_{Ao}\cdot\xi\cdot k_a}{\tau}$$

or in other words:

$$\frac{d^2\cdot\theta}{dt^2} + \left(k_d + k_a + \frac{1}{\tau}\right)\cdot\frac{d\theta}{dt} + \frac{k_d}{\tau}\cdot\theta = \frac{C_{Ao}\cdot\xi\cdot k_a}{\tau} \qquad (3)$$

Equation (3) is a nonhomogenuous second order differential equation with constant coefficients. Its solutions are outlined in "Advanced Engineering Mathmetics" by Wylie and Barrett (see 5th edition, page 98)

$\theta(t)$ = complementary function + particular function.

The characteristic equation of (3) is:

$$m^2 + \left(k_d + k_a + \frac{1}{\tau}\right)\cdot m + \frac{k_d}{\tau} = 0$$

Solution to the above characteristic equation is:

$$m_1 = \frac{-\left(k_d + k_a + \frac{1}{\tau}\right) + \sqrt{\left(k_d + k_a + \frac{1}{\tau}\right)^2 - \frac{4\cdot k_d}{\tau}}}{2}$$

$$m_2 = \frac{-\left(k_d + k_a + \frac{1}{\tau}\right) - \sqrt{\left(k_d + k_a + \frac{1}{\tau}\right)^2 - \frac{4\cdot k_d}{\tau}}}{2}$$

Assume: $\left(k_d + k_a + \frac{1}{\tau}\right)^2 \geq \frac{4\cdot k_d}{\tau}$

So: $m_1 = 0$

$$m_2 = -k_d - k_a - \frac{1}{\tau}$$

Therefore the complementary function is as follows where m_1 and m_2 are expressed above:

$$c_1 + c_2\cdot\exp\left(m_2\cdot t\right)$$

Next step is to find particular integral to complete the solution.

Assumeθ=At^2+Bt+C therefore:

$$\frac{d\theta}{dt}=2At+B$$

$$\frac{d^2\cdot\theta}{dt^2}=2A$$

Plugging into equation (3):

$$2A+\left(k_d+k_a+\frac{1}{\tau}\right)\cdot(2At+B)+\frac{k_d}{\tau}\cdot(At^2+Bt+C)=\frac{C_{Ao}\cdot\xi\cdot k_a}{\tau}$$

From above we can get the following eqations:

$$\frac{k_d}{\tau}\cdot A=0$$

$$\left(k_d+k_a+\frac{1}{\tau}\right)\cdot 2A+\frac{k_d\cdot B}{\tau}=0$$

$$2A+\left(k_d+k_a+\frac{1}{\tau}\right)\cdot B+\frac{k_d\cdot C}{\tau}=\frac{C_{Ao}\cdot\xi\cdot k_a}{\tau}$$

Solve these 3 equtions, we get:

$$A=0$$

$$B=0$$

$$C=\frac{C_{Ao}\cdot\xi\cdot k_a}{k_d}$$

Therefore a particular solution is:

$$\theta=\frac{C_{Ao}\cdot\xi\cdot k_a}{k_d}$$

Therefore the general solutions is thus:

$$\theta=\frac{C_{Ao}\cdot\xi\cdot k_a}{k_d}+c_1+c_2\cdot\exp\left(m_2\cdot t\right) \qquad (4)$$

where c_1 and c_2 are two constants determined by boundary conditions.
The boundary conditions are as follows:

$\theta=\theta_o$ at $t=0$

$\theta=0$ at $t=\infty$

Plugging boundary conditions into (4), we can solve for C_1 and C_2:

$$c_1=\frac{-C_{Ao}\cdot\xi\cdot k_a}{k_d}$$

$$c_2=\theta_o$$

Therefore,$\theta(t)$ is:

$$\theta(t)=\frac{-C_{Ao}\cdot\xi\cdot k_a}{k_d}+\theta_o\cdot\exp\left[-\left(k_d+k_a+\frac{1}{\tau}\right)\cdot t\right] \qquad (5)$$

We need to get a similar expression for C_A. Now plugging equation 4 to equation 1:

$$\frac{dC_A}{dt}+\left(\frac{1}{\tau}+k_a\right)\cdot C_A=\frac{k_d\cdot\theta_o}{\xi}\cdot\exp\left[-\left(k_d+k_a+\frac{1}{\tau}\right)\cdot t\right]+\frac{C_{Ao}}{\tau}-C_{Ao}\cdot k_a \qquad (6)$$

Integrating factor for the above differential equation is :

$$\mu(t)=\exp\left[\left(\frac{1}{\tau}+k_a\right)\cdot t\right]$$

The general solution is as following, where C is a constant:

$$C_A(t)=\mu(t)^{(-1)}\cdot\left[\int \mu(t)\cdot\left[\frac{k_d\cdot\theta_o}{\xi}\cdot\exp\left[-\left(k_d+k_a+\frac{1}{\tau}\right)\cdot t\right]+\frac{C_{Ao}}{\tau}-C_{Ao}\cdot k_a\right]dt+C\right]$$

Solve it and we get:

$$C_A(t)=C_{Ao}\cdot\frac{\frac{1}{\tau}-k_a}{\frac{1}{\tau}+k_a}-\frac{\theta_o}{\xi}\cdot\exp\left[\left(k_a-k_d+\frac{1}{\tau}\right)\cdot t\right]+C\cdot\exp\left[-\left(\frac{1}{\tau}+k_a\right)\cdot t\right]$$

Plugging the boundary condition, $C_A = C_0$ at $t = 0$

$$C_o = C_{Ao} \cdot \frac{\frac{1}{\tau} - k_a}{\frac{1}{\tau} + k_a} - \frac{\theta_o}{\xi} + C$$

Therefore the complete solution is:

$$C_A(t) = C_{Ao} \cdot \frac{\frac{1}{\tau} - k_a}{\frac{1}{\tau} + k_a} - \frac{\theta_o}{\xi} \cdot \exp\left[\left(k_a - k_d + \frac{1}{\tau}\right) \cdot t\right] + \left[C_o - C_{Ao} \cdot \frac{\frac{1}{\tau} - k_a}{\frac{1}{\tau} + k_a} + \frac{\theta_o}{\xi}\right] \cdot \exp\left[-\left(\frac{1}{\tau} + k_a\right) \cdot t\right] \quad (7)$$

DOE F 1332.3
(11-84)

U.S. DEPARTMENT OF ENERGY
MILESTONE SCHEDULE ☐ PLAN ☒ REPORT

FORM APPROVED
OMB 1901-1400

1. TITLE	2. REPORTING PERIOD	3. IDENTIFICATION NUMBER
ISOBUTANOL METHANOL MIXTURE FROM SYNGAS	Oct. 1, 1996 - Dec. 31, 1996	DE - AC22 - PC94PC066

4. PARTICIPANT NAME AND ADDRESS	5. START DATE	6. COMPLETION DATE
Department of Chemical Engineering University of California - Berkeley	Oct 1994	Sept 1997

7. ELEMENT CODE	8. REPORTING ELEMENT	9. DURATION 94 ← 95 → ← 96 → ← 97 → Q1 Q2 Q3 Q4 Q1 Q2 Q3 J A S O N D J F M A M J J A S	10. PERCENT COMPLETE a Plan	b Actual
	Task 4	Identify reaction intermediates by TPSR and high pressure infrared methods	75	75
	Tasks 3 & 5	Identify catalysts with highest isoalcohol yields (two) and evaluate at conditions resembling envisioned commercial practice.	80	80
	Task 5	Assess economic viability of these catalytic materials	65	NA
	Task 5	Complete testing of at least two selected catalysts in slurry reactors.	65	0
	Tasks 3 & 5	Choose two materials for detailed studies of the reaction mechanism and of optimum synthetic protocols	50	50
	Tasks 3 & 5	Complete mechanistic studies on most promising materials	0	0
	Tasks 2 & 5	Develop synthetic procedures that can be carried out on a commercial scale Suggest a range of catalyst compositions for future study.	0	0
	Task 5	Complete testing of the two selected catalytic materials	0	0
	Task 5	Assess future research requirements, technical readiness and economic viability of the most promising approach	0	0
		Produce final report	0	0

DOE F 1332.3
(11-84)

U.S. DEPARTMENT OF ENERGY
MILESTONE SCHEDULE ☐ PLAN ☒ REPORT

FORM APPROVED
OMB 1901-1400

1. TITLE	2. REPORTING PERIOD	3. IDENTIFICATION NUMBER
ISOBUTANOL METHANOL MIXTURE FROM SYNGAS	Oct. 1, 1996 - Dec. 31, 1996	DE - AC22 - PC94PC066

4. PARTICIPANT NAME AND ADDRESS	5. START DATE	6. COMPLETION DATE
Department of Chemical Engineering University of California - Berkeley	Oct 1994	Sept 1997

7. ELEMENT CODE	8. REPORTING ELEMENT	9. DURATION	10. PERCENT COMPLETE a Plan	b Actual
	Task 3	Complete design, construction and start-up of packed bed reactor module	100	100
	Task 2	Prepare Cu-based catalyst compositions and characterize structure, surface area, and effectiveness of several synthetic approaches	100	100
	Task 2	Choose four promising materials for catalyst evaluation	100	100
	Task 3	Construct recirculating reactor module Establish reaction pathways and rate-determining steps	100	100
	Tasks 2 & 3	Identify catalyst components necessary to catalyze rate-determing steps that have been determined	100	100
	Tasks 2 & 3	Identify synthetic techniques to increase the reactivity and accessibility of such required sites	100	100
	Task 4	Complete construction and start-up of temperature programmed surface reaction apparatus and design of high-pressure infrared cell	100	100
	Task 4	Design and construction of high-pressure infrared cell	100	100
	Task 4	Calibrate between UCB and APCI laboratories by testing two selected catalysts	100	100
	Task 2	Determine the density and reactivity of the required sites and implement synthetic methods to improve them	80	75

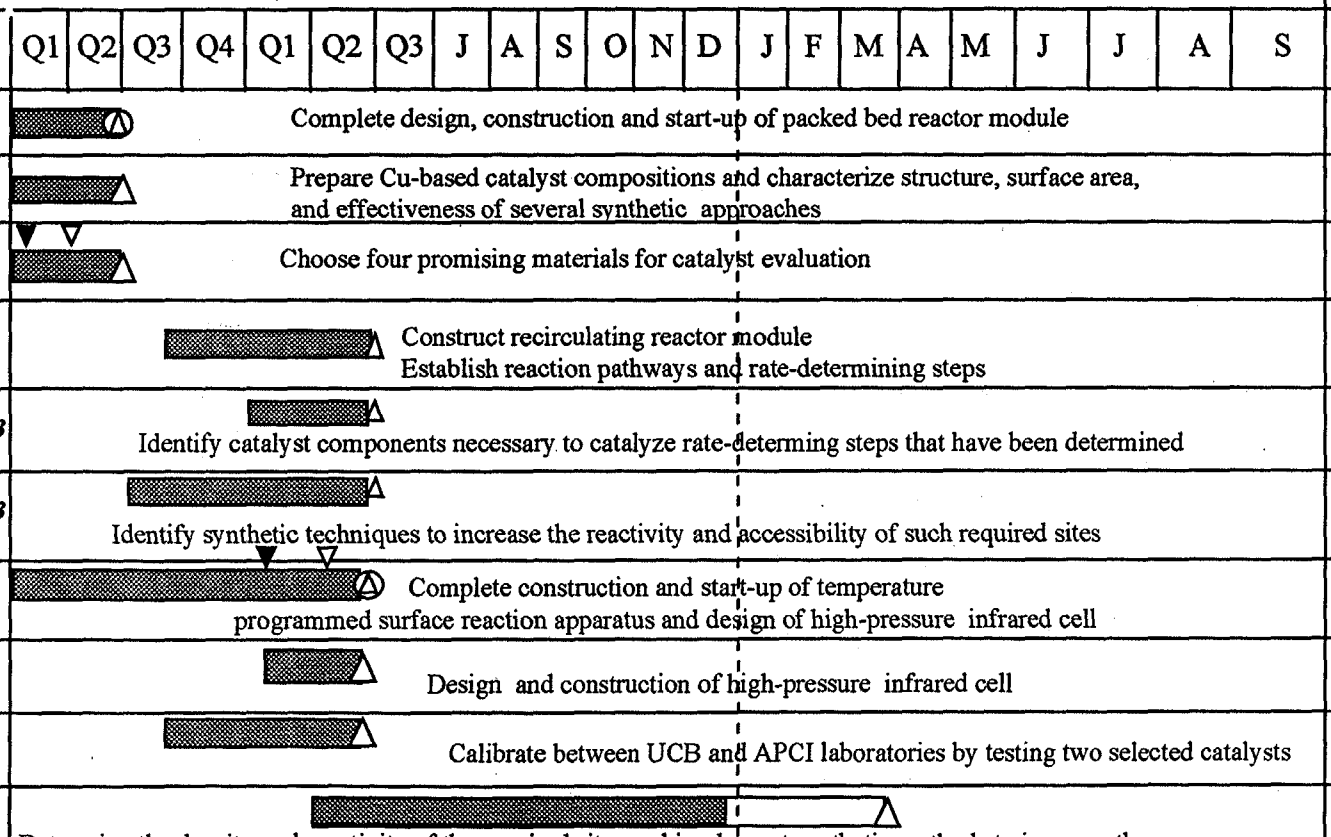

1. TITLE ISOBUTANOL- METHANOL MIXTURE FROM SYNGAS					2. REPORTING PERIOD October 1, 1996 to Dec. 31, 1996						3. IDENTIFICATION NUMBER DE-AC22-PC94PC066		
2. PARTICIPANT NAME AND ADDRESS Department of Chemical Engineering University of California- Berkeley, Berkeley, CA 94720					5. COST PLAN DATE Jan. 27, 1997						6. START DATE OCT 1994 7. COMPLETION DATE OCT 1997		
8. Element code	9. Reporting element	ACCRUED COSTS				ESTIMATED ACCRUED COSTS						12. Total contract Value	13. Variance
		Reporting period		Cumulative to date		a.total this fiscal year	b. balance of fiscal year	c. FY96 (1)	d. FY 97 (2)	(3)	e. total		
		a. Actual	b. Plan	c. Actual	d. Plan								
	1. Total (Direct material)	10,955	22,777	86,940	165,152	10,955	80,154	91,109	94,782		261,876	259,929	-1,947
	a) Purchased Parts	10,955	9,106	77,039	110,468	10,955	25,470	36,425	40,200		142,709	98,175	-44,534
	b) Subcontracted Items	0	13,670	3,970	128,722	0	54,679	54,679	54,582		113,231	161,754	48,523
	c) Other	0	0	5,931	74,043	0	0	0	0		5,931	0	-5,931
	2. Material Overhead	0	0	0	0	0	0	0	0		0	0	0
	3. Direct Labor 'Total	10,951	20,892	128,611	163,921	10,951	72,618	83,569	92,812		294,041	256,725	-37,316
	4. Labor Overhead	0	0	0	0	0	0	0	0		0	0	0
	5. Fringe Benefits	866	3,350	14,787	26,168	866	12,534	13,400	15,368		42,689	41,538	-1,151
	6. Special Testing	88	0	2,799	0	88	0	0	0		2,799	0	-2,799
	7. Special Equipment	0	2,000	290,137	260,000	0	8,000	8,000	0		298,137	260,000	-38,137
	8. Travel	421	1,629	7,339	12,720	421	6,094	6,515	7,020		20,453	19,740	-713
	9. Consultants	0	0	0	0	0	0	0	0		0	0	0
	10. Other Direct costs	0	6,114	0	47,745	0	24,455	24,455	25,677		50,132	73,422	23,290
	11. Direct costs and Overhead	23,280	56,761	530,613	675,702	23,280	203,764	227,044	235,653		970,030	911,354	-58,676
	12. General and Administrative Expense '49.5 %	11,617	20,505	119,886	165,757	11,617	70,403	82,020	90,358		280,646	256,108	-24,538
	13. Facilities Capital Cost of Money	0	0	0	0	0	0	0	0		0	0	0
	14. Total Estimated Cost	34,897	77,266	650,499	841,457	34,897	274,165	309,062	326,008		1,250,672	1,167,462	-83,210
	15. Fee	0	0	0	0	0	0	0	0		0	0	0
	16. Cost Sharing	0	9,949	205,766	252,851	0	39,797	39,797	56,789		302,352	301,651	-701
	17. Total estimated DOE funds spent = Item 14-Item 16	34,897	67,316	444,733	588,606	34,897	234,368	269,265	269,219		948,320	865,811	-82,509
14. Total		34,897	67,316	444,733	588,606	34,897	234,368	269,265	269,219		948,320	865,811	-82,509

15. DOLLARS EXPRESSED IN One U.S. Dollar	16. SIGNATURE OF PARTICIPANT PROJECT MANAGER AND DATE	17. SIGNATURE OF PARTICIPANT'S AUTHORIZED FINANCIAL SERVICE REPRESENTATIVE AND DATE Lourdes S. Farrer 1/27/97